Suspended, Straightened Carbon Nanotube Arrays by Gel Chapping

Chunyan Ji,[†] Hongbian Li,[†] Luhui Zhang,[†] Yu Liu,[‡] Yan Li,[‡] Yi Jia,[§] Zhen Li,[§] Peixu Li,[§] Enzheng Shi,[†] Jinquan Wei,[§] Kunlin Wang,[§] Hongwei Zhu,[§] Dehai Wu,[§] and Anyuan Cao[†,*]

[†]Department of Advanced Materials and Nanotechnology, College of Engineering, Peking University, Beijing 100871, P. R. China, [‡]Beijing National Laboratory for Molecular Sciences, National Laboratory of Rare Earth Material Chemistry and Application, Key Laboratory for the Physics and Chemistry of Nanodevices, College of Chemistry and Molecular Engineering, Peking University, Beijing 100871, China, and [§]Key Laboratory for Advanced Materials Processing Technology and Department of Mechanical Engineering, Tsinghua University, Beijing 100084, P. R. China

ABSTRACT We report large-scale self-assembly of suspended, straightened, single-walled carbon nanotubes (SWNTs) across regular TiO_2 gel islands. By coating a SWNT network on top of a pool of the TiO_2 colloid and inducing a rapid drying and chapping process, initially curled, random SWNTs can be straightened into aligned arrays and suspended across the island gaps. The suspended SWNT arrays were grafted by semiconducting or metallic nanoparticles, resulting in hybrid structures with tailored and neat morphology, and enhanced photoresponse. We further demonstrate these suspended SWNTs can sustain high speed gas blowing (up to 20 m per second) reversibly for hundreds of cycles, and detect gas velocity by the resistance change.

KEYWORDS: carbon nanotube · suspended array · self-assembly · photodetector · flow sensor

Carbon nanotubes are unique one-dimensional structures combining high mechanical strength, flexibility, and electrical conductivity. Nanotubes, when suspended, can be manipulated by many ways and constructed as nanoelectromechanical systems coupling mechanical, electrical, thermal and optical responses.[1] In the past years, many systems based on multiwalled or single-walled nanotubes (SWNTs) have been built and exhibited fascinating properties, such as tunable oscillators,[2−4] rotational actuators,[5] cargo and mass conveyors,[6,7] and torsional pendulums.[8] To ensure high performance and stability, an important requirement in device fabrication is that the nanotubes must be suspended away from the substrate with both ends fixed safely, and the suspended portion should not be loose. For suspended devices based on nanotubes or graphene ribbons, improved signal-to-noise ratio can be obtained which allow detail study on the electronic or electromechanical properties of those nanostructures.[9−11] Although devices based on individual nanotubes have met great success, fabrication of large-scale suspended, stable SWNT structures remains challenging.[12] Common methods involve depositing individual SWNTs across prefabricated trenches or etching the substrate region underneath a SWNT to form a trench, and the latter usually involves a number of complex lithography steps.[1−8] In addition, anchoring of the SWNT ends only relies on the adhesion to the oxide surface or metal electrodes, which might not be strong enough to lift cargos or excite resonant vibrations.[2,7]

Recently, researchers directly grew horizontally aligned SWNTs with centimeter length by controlling their interaction with substrates and the gas flow condition during chemical vapor deposition process.[13,14] Also, self-assembly methods such as dielectrophoresis and blown bubble film techniques produced densely packed SWNT arrays bridging electrode pairs, or parallel SWNTs in a fluid bubble film.[15,16] However, most of the previous methods yielded SWNTs resting on the substrate surface or embedded in a polymer matrix, that are not suitable for making suspended electromechanical systems.

Here, we show that large-area suspended, straight SWNT arrays can be obtained by a self-assembly method utilizing a gel chapping phenomenon, in which a pool of gel cracks into separate islands upon drying. We have reported synthesis of 100 cm^2 free-standing thin films consisting of randomly interconnected SWNTs and bundles (Figure 1a).[17] A piece of such film was transferred to the top of a droplet of TiO_2 colloid in a semisolid state. It seems that the ethanol-based colloid can wet the SWNT film and partially infiltrate into its porous network, which ensures a strong interaction between the colloid and SWNTs. This interaction is important for grabbing and stretching SWNTs later. The SWNT-covered TiO_2 gel was heated rapidly in vacuum to dry the gel, during which the gel chapped into small

* Address correspondence to anyuan@pku.edu.cn.

Received for review April 7, 2011 and accepted June 23, 2011.

Published online June 23, 2011
10.1021/nn2012805

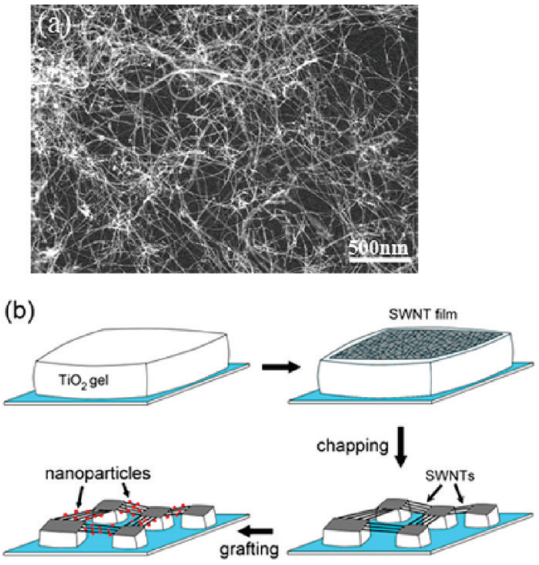

Figure 1. Gel chapping process and suspending of SWNTs. (a) SEM image of a pristine SWNT film consisting of random, curled nanotubes. (b) Illustration of the gel chapping process and simultaneous suspending and straightening of the SWNTs on the top. The resulting SWNT arrays can be further grafted by nanoparticles to form a hybrid structure.

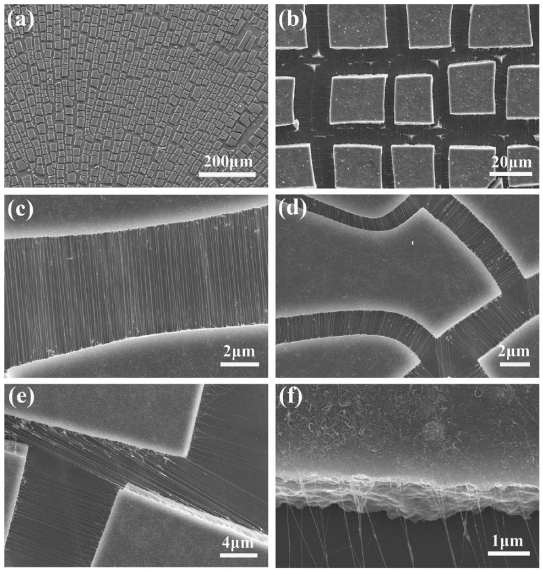

Figure 2. Suspended SWNT arrays across gel islands: (a) SEM image of a large-area chapped TiO_2 islands; (b) rectangular shaped islands with gap distances up to 20 μm; (c) straightened SWNT arrays across a trench; (d) an area where linear and curved trenches are filled with aligned SWNTs; (e) SWNTs stretched between adjacent islands; (f) close view near the edge of gel islands.

islands (10−100 μm in width) and simultaneously suspended and straightened the SWNTs on the top. The resulting SWNTs hanging between adjacent islands can serve as a platform for making hybrid arrays by grafting nanoparticles. The self-assembly process is illustrated in Figure 1b.

Figure 2a shows the scanning electron microscopy (SEM) image of a large-area chapped TiO_2 gel islands on a silicon oxide substrate. We obtained relatively uniform distribution of separate islands with a rectangular block-like shape by controlled heating and drying of the gel (see Methods for details). In a more regular region, microscale islands with sharp edges and widths of tens of micrometers were formed by the cracking and moving apart of the gel, leaving gap distances of 1−20 μm (Figure 2b). It might be possible to obtain large-area gel islands with controlled shape, size, and distribution, by photolithography patterning of the substrate or the starting sol−gel material as well as controlling the drying and chapping temperature (square-shaped islands were produced at about 60 °C). Close view shows aligned SWNT arrays hanging across all the trenches, and most SWNTs are perpendicular to the edge of the island (Figure 2c,d). In some cases we observed river-like curved trenches formed between irregular islands which are also filled with aligned SWNTs (Figure 2d). The linear density of aligned SWNTs (and small bundles) is about 1−10 bundle/μm, and can be changed by the thickness of the pristine film at the beginning stage. The SWNTs in the film have lengths of at least tens of micrometers and can bridge adjacent islands continuously. Although there are some impurities present in the initial film, the exposed SWNT arrays in the gap appear much cleaner. We believe most of impurity particles have been removed by the gel during chapping. Occasionally, we found tilted arrays connecting the trench which infer the relative movement between adjacent islands during gel cracking (Figure 2e). Near the cliffs, we can see that the SWNT film resting on the gel surface remains random, and the aligned SWNTs are indeed hanging on top of the trenches (suspended) (Figure 2f).

Our results indicate that the SWNTs are firmly anchored on the TiO_2 islands, and in the trenches they are stretched into straight, aligned arrays. Therefore it is possible that some of the SWNTs are still under axial strains. Raman spectra recorded on different positions in one of the trenches reveal various radial breathing mode peaks in 100 to 300 cm^{-1}, corresponding to SWNTs with different diameters (Figure 3a). At the same time, we frequently see a modest shift of G-band accompanied by the change in line shape (Figure 3b). In comparison, Raman spectrum recorded on pristine random SWNT films always shows a pronounced G-band centered at about 1590 cm^{-1} without much shifting and splitting (Supporting Information Figure S1). According to previous studies on SWNTs under axial strains, the changes in G band position and profile would depend on the structure and were normally more distinct than the changes of RBM when the strain is modest.[18−21] The G_+ and G_- would shift to lower wave numbers under axial strain.[18−20] For metallic SWNTs, the intensity of G_- or G_{BWF} would be remarkably increased and even became higher than that of G_+.[19,20] We can see all such changes of the G-band for

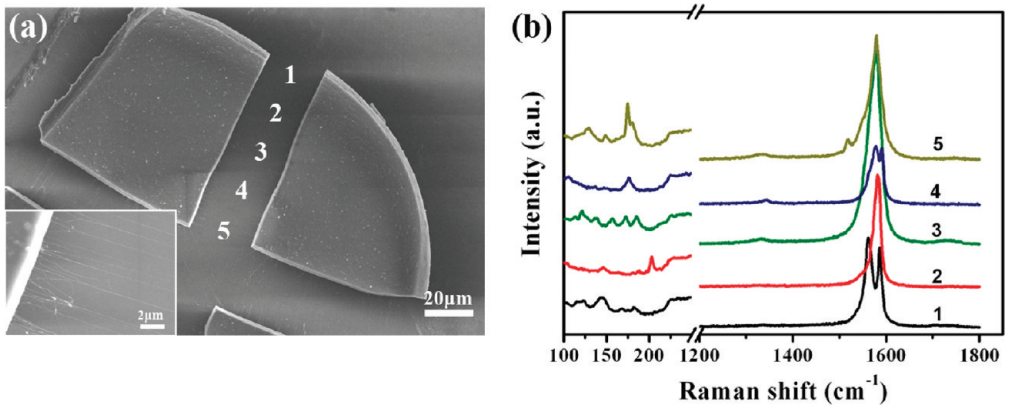

Figure 3. Raman characterization of straightened SWNTs across trenches. (a) SEM image of two gel islands with SWNTs stretched inside the trench. Inset, aligned SWNTs in this trench. (b) Raman spectra recorded at different positions along the trench (labeled as 1−5).

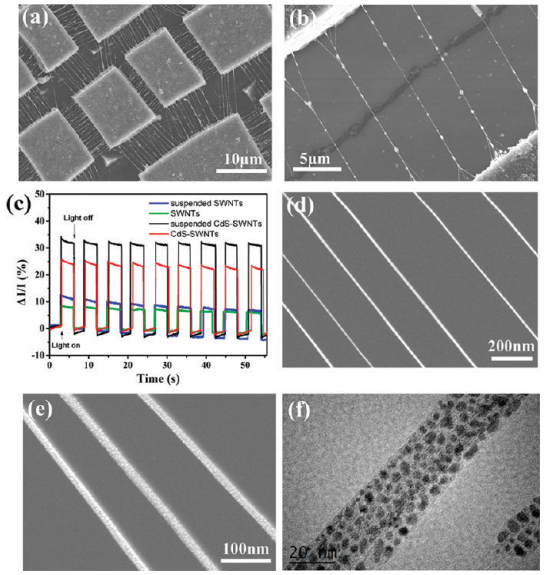

Figure 4. Hybrid SWNT arrays grafted by CdS or Au nanoparticles, and photoresponse: (a) solution processing of the SWNT arrays resulted in thick bundles; (b) close view showing CdS nanoparticles and small aggregates adhered on SWNT bundles; (c) photoresponse (change of current flow under illumination) curves of suspended CdS-SWNT films and three control samples, including unsuspended CdS-SWNT film (red curve), suspended SWNT films without nanoparticles (blue), and unsuspended SWNT films (green); (d) SEM image of pristine, clean SWNT arrays; (e) SWNT arrays after Au plasma sputtering where white contrast dots (Au nanoparticles) can be seen on each bundle; (f) transmission electron microscopy (TEM) image of Au-grafted SWNT bundles showing well-dispersed Au nanoparticles (diameter of 2−5 nm) along the bundle surface.

SWNTs suspended on the trenches as shown in Figure3b. This indicates that the cracking and retreating of gel islands can exert axial stress on SWNTs, resulting in straightened arrays between the islands.

Our suspended SWNT arrays can serve as a platform for building optoelectronic systems and flow sensors through collective action. Considering the electronic interaction between SWNTs and semiconducting nanoparticles,[22,23] we fabricated a suspended hybrid structure by grafting 5 nm CdS nanoparticles onto the surface of SWNTs through a solution method (Figure 4a,b). After solvent evaporation, the SWNTs condensed into thicker bundles attached by CdS aggregates along the span over the trench. The CdS nanoparticles were grafted to the island surface as well. Because chapped gel islands are well connected by SWNT arrays, the entire SWNT film remains electrically conductive. We have tested the photoresponse of a piece of assembled SWNT array containing hundreds of TiO_2 islands. Under simulated light illumination at AM1.5, 100 mW/cm^2, and a set bias of 1 V, the pristine SWNT film and arrays assembled on gel islands show current increases by ~8% to 11% upon illumination. Under the same condition, the suspended CdS-SWNT arrays show significantly enhanced current increase by more than 32% (Figure 4c), owing to the electron injection from the conduction band of CdS nanoparticles (and a small contribution from TiO_2 nanoparticles) to SWNTs.[22] In comparison, unsuspended CdS-SWNT films show reduced photoresponse with a current increase of <25%. The results show a modest enhancement of photoresponse by suspending CdS-SWNT films. Similar enhancement of photocurrent in CdS-SWNT films due to charge transfer has been reported in a previous work.[23] The photoresponse of both SWNT arrays and their hybrids is reversible and reliable over many cycles. In addition to CdS, other nanoparticles (*e.g.*, Au) also can be grafted to the SWNT arrays. Using plasma sputtering, we obtained very fine Au nanoparticles (about 2−5 nm) uniformly attached to the SWNT bundles, forming a neat hybrid array (Figure 4d−f).

The suspended SWNT arrays allow direct gas blowing along the normal direction to the array plane. Downward Ar gas blowing at controlled rate was introduced to pass through the aligned SWNTs across TiO_2 islands, and a two-probe configuration was used to monitor the current change (ΔI) through the whole film (Figure 5a, Supporting Information, Figure S2). *In situ* observation by optical microscope reveals that the

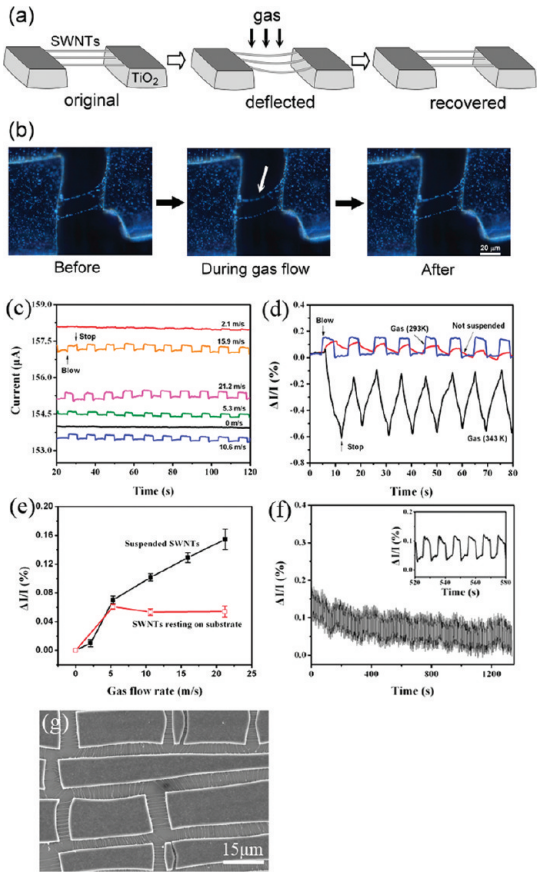

Figure 5. Gas flow sensor based on suspended SWNT arrays. (a) Illustration of the SWNT arrays between islands which deflect during gas flow and recover to straight shape after stopping gas. (b) Optical images of two SWNT bundles (attached by CdS nanoparticles for clear imaging) before, during, and after Ar gas flow. The white arrow in middle panel points to the deflection of SWNTs. (c) Recorded current change through the SWNT film during cycled gas blowing at various velocities from 0 (without blowing) up to 21.2 m/s. There is a little fluctuation in the initial current level (153−158 μA) for each velocity gas blowing test. (d) Current change for samples including SWNT films coated on substrate surface (not suspended), suspended SWNT arrays in room temperature gas flow (293 K), and suspended SWNTs in high temperature gas flow (343 K) at the same velocity (10.6 m/s). (e) Relative current increase ($\Delta I/I$) as a function of gas flow rate, showing a linear relationship in suspended SWNTs. (f) Current change in suspended SWNTs during repeated gas blowing for more than 200 cycles. Inset shows stable and reversible current increase during each cycle. (g) SEM image of SWNT arrays suspended between gel islands after gas blowing for 200 cycles.

suspended SWNTs were deflected into an arc shape during Ar gas blowing at a calculated velocity of 10.6 m/s (500 sccm through 1 mm diameter capillary), and recovered to original straight morphology after the blowing was stopped (Figure 5b). At a set bias of 1 V, the SWNT film (including suspended arrays) was heated by a constant current of 154 μA. When gas flow was introduced in perpendicular to the film, suspended portions work like hot-wires which were cooled down in gas flow, resulting in a decrease of resistance and increase of current flow (by about 0.1%). We can see fast and regular increase and drop of current in cycles of gas blowing at velocities ranging from 2.1 m/s up to 21.2 m/s (Figure 5c). A few factors may contribute to the resistance change of SWNTs in gas flow, including the SWNT deflection, gas cooling effect, and even gas adsorption onto SWNTs. When mixed semiconducting and metallic SWNTs are deflected, their conductivities could change in different ways (increase or decrease) depending on electronic properties. It was found that metallic tubes showed increased resistance or no significant change during stretching.[24] Here, SWNT deflection does not induce major resistance change as compared to gas cooling. In addition, although both SWNTs suspended in the gaps and coated on the island surface are subjected to the gas flow, the resistance change in the gap region should dominate the entire film. The suspended SWNTs are less dense compared to the random film on gel islands, and therefore can be completely surrounded by gas flow, resulting in more effective cooling. Attaching a thermocouple to the SWNT film reveals a temperature drop of about several centigrade degrees during gas blowing.

To confirm the temperature effect, Ar gas was heated to higher temperature (70 °C), and then allowed to flow through the SWNT arrays at the same velocity (10.6 m/s). This time we observed a decrease of current during hot gas flow ($\Delta I/I \approx -0.6\%$), indicating that the SWNTs are heated (instead of cooled) and their resistance increases correspondingly (Figure 5d). It was found that Joule heating a SWNT film in Ar resulted in a small increase of sheet resistance.[25] For a pristine SWNT film adhering to a silicon oxide substrate (without being suspended), we observed reduced current increment and relatively slower response without flat region (stable current) during gas flow (Figure 5d). Therefore suspending SWNTs is important for obtaining quick and reliable response to gas flow. Moreover, in suspended arrays, the current change shows a nearly linear relationship depending on the gas velocity, which is about 0.07% at a velocity of 5.3 m/s, and increases to 0.16% at higher velocity (21.2 m/s) (Figure 5e). In comparison, the SWNT film lying on the substrate does not show such relationship and cannot detect the velocity change of gas flow (Figure 5e).

The suspended SWNT arrays are very robust and can sustain gas blowing for more than 200 cycles without degradation of current response (Figure 5f). After that, SEM characterization reveals well-maintained SWNT arrays across trenches, although some bundles appear slight loose (Figure 5g). The mechanical strength and flexibility make SWNTs ideal structures for constructing durable gas flow sensors. For practical use in different gas flow, one has to consider conductance change caused by interaction between certain reactive gas molecules (*e.g.*, oxygen) and SWNTs. It might be possible to sheath suspended SWNTs with an inert metal shell or

wrap the SWNTs by appropriate organic molecules in order to prevent direct exposure to reactive gas.

In conclusion, a gel chapping process was utilized to simultaneously suspend and straighten carbon nanotubes across gel islands. The method is applicable to various one-dimensional structures as well as other types of sol−gel materials, and can be scaled up to make large-area suspended structures. Owing to the flexibility and robustness of nanotubes, our suspended SWNT arrays and their hybrids have potential applications in photodetectors, gas or fluid sensors, and integrated nanoelectromechanical systems.

METHODS

Synthesis of SWNT Films. Large area, thin films of single-walled carbon nanotubes were synthesized by chemical vapor deposition (CVD) using xylene and ferrocene as carbon source and catalyst precursor, respectively, with a small amount addition of sulfur. Ferrocence was dissolved into xylene at a concentration of 0.045 g mL^{-1} and then mixed with sulfur powders at a concentration of 0.001 g mL^{-1} to form a solution. The mixture was injected into the furnace (upstream, 200 °C) at a feeding rate of 3−5 μL min^{-1} by an automatic syringe pump. The vapor was carried to the reaction zone by a gas mixture of argon and hydrogen flowing at 1500 sccm (volume ratio of Ar/H_2 is equal to 0.85:0.15). Reaction zone temperature was set at 1150−1170 °C for favorable growth of single-walled nanotubes. Typical growth time is 30 min. SWNT films were collected by flexible nickel foil substrates clinging to the inner wall of the quartz tube in the downstream low-temperature side.

Synthesis of CdS Nanoparticles. One mmol of $CdCl_2 \cdot 5H_2O$ was dissolved in 10 mL of oleylamine and then heated at 175 °C for 20−35 min under argon flow. Then a solution of sulfur dissolved in oleylamine-sulfur (1.2 M) was injected into the hot reaction mixture under gentle stirring. The reaction mixture was held at 175 °C and stirred for ~3 h. At last, a large volume of toluene was injected into the product to quench the reaction and cool down to room temperature. The as-synthesized CdS nanoparticles with diameters of 4−6 nm were rinsed by ethanol/hexane repeatedly to remove organic molecules wrapping on the particles.

Synthesis of TiO_2 Colloid. About 5 mL of $Ti(OBu)_4$, 23 mL of ethanol, and 0.5 mL of ethyl acetate were mixed in a flask as precursors. Then a hydrolysate solution containing 1.5 mL of HNO_3 (0.1M), 1.5 mL of deionized water, and 12 mL of ethanol was added by droplets into the precursor solution at a rate of 0.5−1 mL/min. The mixture was stirred continuously for 12 h (800 r/min) and then aged for 12 h at room temperature.

Assembly of Suspended SWNT Arrays on TiO_2 Gel Islands. The TiO_2 colloid was centrifuged at a rotation rate of 4000 rev/min for 5 min, and then the supernatant consisting of relatively small and uniformly dispersed TiO_2 nanoparticles was used for making the gel and chapping. The supernatant was coated onto a glass sheet or silicon oxide wafer to form a thick semisolid mesa about 1 cm^2 in area. On the mesa, a pristine film consisting of random SWNTs was gently coated to allow wetting and contact between SWNTs and wet gel. This assembly was placed in a vacuum oven and heated to 60 °C for 10 min, during which the TiO_2 gel completely dried and chapped into microscale islands with stretched SWNTs suspended across those islands. The island shape (rectangular) and distribution is more regular than the sample chapped at a lower temperature (20 °C).

Grafting CdS and Au Nanoparticles onto SWNT Arrays. As-synthesized CdS powder was dispersed and diluted in tetrahydrofuran (THF) solution (0.094 M). The assembled SWNTs-on-TiO_2 islands were immersed into the solution for 12 h without stirring or heating, to allow CdS nanoparticles attach to the SWNT surface. Then the sample was picked out and rinsed in ethanol to remove redundant nanoparticles from the sample surface. During solvent evaporation, the SWNT arrays condense into thicker bundles grafted by small aggregates of CdS nanoparticles. Au nanoparticles were deposited onto SWNT arrays by plasma sputtering at a set current of 5 mA and time of 2 min, which results in uniformly distributed ~2 nm particles along the SWNT bundles.

Photoresponse and Gas Blowing Tests on SWNT Arrays. The hybrid CdS-SWNT arrays supported by TiO_2 islands were used for tests. We made a simple two-terminal device configuration by connecting Ag wire electrodes to the two sides of SWNT film spanning all the islands. The distance between two electrodes was usually set at about 2−4 mm spanning over tens of TiO_2 microislands. Simulated light (AM 1.5, 100 mW/cm^2) was illuminated to the entire sample for a set time and on−off cycles, and the current flow through electrodes was monitored simultaneously. For gas blowing tests, a plastic baffle with a circular hole (diameter = 2 mm) was placed above the two−terminal device. A capillary with inner diameter of 1 mm served as a gas pipe to direct gas flow to the device from a flow meter at controlled flow rate of 0−1500 sccm. The capillary was held vertically and perpendicular to the sample surface, with a small distance of about 5 mm. The actual area in the sample subjected to gas blowing was slightly larger than the capillary diameter due to gas diffusion when it flows out of the capillary, which covers most of chapped gel islands. Cycled gas blowing was performed by periodically blocking and opening the baffle hole at 5 s interval.

SWNT films, nanoparticles, hybrids and devices were characterized by SEM (Hitachi S-4800), TEM (F30), optical microscope (Olympus BX51M) and UV−vis spectroscopy (Lambda 35). Raman spectra were collected on a Jobin Yvon LabRam HR 800 micro-Raman spectrometer with an excitation wavelength of 632.8 nm. A 100× air objective was used, and the spot size was about 1 μm^2. Photoresponse tests were carried out using a solar simulator (Newport 91195) at a calibrated AM1.5, 100 mW·cm^{-2} illumination intensity. The argon (purity >99.99%) flow rate was controlled by a gas flow meter (Sevenstar D08-3F). Electrical measurements on the devices were done using a Keithley 2400 source meter.

Acknowledgment. We thank Prof. X. Guo and Ms. Y. Cao from College of Chemistry in Peking University for help in photomeasurements. This work is supported by the National Science Foundation of China under Grant No. 51072005, NSFC 50972067, and Research Fund for Doctoral Program of Ministry of Education of China (No. 20090002120019). Y. Li acknowledges the Ministry of Science and Technology of China (Project No. 2011CB933003).

Supporting Information Available: Raman spectra of pristine unstretched SWNT films (Figure S1), electrical configuration of suspended SWNT films for photoresponse and gas blowing measurements (Figure S2). This material is available free of charge *via* the Internet at http://pubs.acs.org.

REFERENCES AND NOTES

1. Tombler, T. W.; Zhou, C. W.; Alexseyev, L.; Kong, J.; Dai, H. J.; Lei, L.; Jayanthi, C. S.; Tang, M. J.; Wu, S. Y. Reversible Electromechanical Characteristics of Carbon Nanotubes Under Local-Probe Manipulation. *Nature* **2000**, *405*, 769–772.
2. Sazonova, V.; Yaish, Y.; Ustünel, H.; Roundy, D.; Arias, T. A.; McEuen, P. L. A Tunable Carbon Nanotube Electromechanical Oscillator. *Nature* **2004**, *431*, 284–287.
3. Lassagne, B.; Tarakanov, Y.; Kinaret, J.; Garcia-Sanchez, D.; Bachtold, A. Coupling Mechanics to Charge Transport in Carbon Nanotube Mechanical Resonators. *Science* **2009**, *325*, 1107–1110.
4. Wang, Z. H.; Wei, J.; Morse, P.; Dash, J. G.; Vilches, O. E.; Cobden, D. H. Phase Transitions of Adsorbed Atoms on the

Surface of a Carbon Nanotube. *Science* **2010**, *327*, 552–555.
5. Fennimore, A. M.; Yuzvinsky, T. D.; Han, W.-Q.; Fuhrer, M. S.; Cumings, J.; Zettl, A. Rotational Actuators Based on Carbon Nanotubes. *Nature* **2003**, *424*, 408–410.
6. Regan, B. C.; Aloni, S.; Ritchie, R. O.; Dahmen, U.; Zettl, A. Carbon Nanotubes as Nanoscale Mass Conveyors. *Nature* **2004**, *428*, 924–927.
7. Barreiro, A.; Rurali, R.; Hernández, E. R.; Moser, J.; Pichler, T.; Forró, L.; Bachtold, A. Subnanometer Motion of Cargoes Driven by Thermal Gradients along Carbon Nanotubes. *Science* **2008**, *320*, 775–778.
8. Meyer, J. C.; Paillet, M.; Roth, S. Single-Molecule Torsional Pendulum. *Science* **2005**, *309*, 1539–1541.
9. Cao, J.; Wang, Q.; Rolandi, M.; Dai, H. Aharonov-Bohm Interference and Beating in Single-Walled Carbon-Nanotube Interferometers. *Phys. Rev. Lett.* **2004**, *93*, 216803/1–216803/4.
10. Cheng, Z.; Li, Q.; Li, Z.; Zhou, Q. Y.; Fang, Y. Suspended Graphene Sensors with Improved Signal and Reduced Noise. *Nano Lett.* **2010**, *10*, 1864–1868.
11. Hod, O.; Scuseria, G. E. Electromechanical Properties of Suspended Graphene Nanoribbons. *Nano Lett.* **2009**, *9*, 2619–2622.
12. Hayamizu, Y.; Yamada, T.; Mizuno, K.; Davis, R. C.; Futaba, D. N.; Yumura, M.; Hata, K. Integrated Three-Dimensional Microelectromechanical Devices from Processable Carbon Nanotube Wafers. *Nat. Nanotechnol.* **2008**, *3*, 289–294.
13. Jin, Z.; Chu, H. B.; Wang, J. Y.; Hong, J. X.; Tan, W. C.; Li, Y. Ultralow Feeding Gas Flow Guiding Growth of Large-Scale Horizontally Aligned Single-Walled Carbon Nanotube Arrays. *Nano Lett.* **2007**, *7*, 2073–2079.
14. Kang, S. J.; Kocabas, C.; Ozel, T.; Shim, M.; Pimparkar, N.; Alam, M. A.; Rotkin, S. V.; Rogers, J. A. High-Performance Electronics using Dense, Perfectly Aligned Arrays of Single-Walled Carbon Nanotubes. *Nat. Nanotechnol.* **2007**, *2*, 230–236.
15. Shekhar, S.; Stokes, P.; Khondaker, S. I. Ultrahigh Density Alignment of Carbon Nanotube Arrays by Dielectrophoresis. *ACS Nano* **2011**, *5*, 1739–1746.
16. Yu, G.; Cao, A.; Lieber, C. M. Large-Area Blown Bubble Films of Aligned Nanowires and Carbon Nanotubes. *Nat. Nanotechnol.* **2007**, *2*, 372–377.
17. Li, Z.; Jia, Y.; Wei, J.; Wang, K.; Shu, Q.; Gui, X.; Zhu, H.; Cao, A.; Wu, D. Large Area, Highly Transparent Carbon Nanotube Spiderwebs for Energy Harvesting. *J. Mater. Chem.* **2010**, *20*, 7236–7240.
18. Cronin, S. B.; Swan, A. K.; Unlü, M. S.; Goldberg, B. B.; Dresselhaus, M. S.; Tinkham, M. Resonant Raman Spectroscopy of Individual Metallic and Semiconducting Single-Wall Carbon Nanotubes under Uniaxial Strain. *Phys. Rev. B* **2005**, *72*, 035425/1–035425/8.
19. Cronin, S. B.; Swan, A. K.; Unlü, M. S.; Goldberg, B. B.; Dresselhaus, M. S.; Tinkham, M. Measuring the Uniaxial Strain of Individual Single-Wall Carbon Nanotubes: Resonance Raman Spectra of Atomic-Force-Microscope Modified Single-Wall Nanotubes. *Phys. Rev. Lett.* **2004**, *93*, 167401/1–167401/4.
20. Liu, Z. F.; Zhang, J.; Gao, B. Raman Spectroscopy of Strained Single-Walled Carbon Nanotubes. *Chem. Commun.* **2009**, 6902–6918.
21. Wang, J. Y.; Cui, R. L.; Liu, Y.; Zhou, W. W.; Jin, Z.; Li, Y. Abnormal Raman Intensity of Single-Walled Carbon Nanotubes Grown on Silica Spheres. *J. Phys. Chem. C* **2009**, *113*, 5075–5080.
22. Robel, I.; Bunker, B. A.; Kamat, P. V. Single-Walled Carbon Nanotube–CdS Nanocomposites as Light-Harvesting Assemblies: Photoinduced Charge-Transfer Interactions. *Adv. Mater.* **2005**, *17*, 2458–2463.
23. Li, X. L.; Jia, Y.; Cao, A. Tailored Single-Walled Carbon Nanotube–CdS Nanoparticle Hybrids for Tunable Optoelectronic Devices. *ACS Nano* **2010**, *4*, 506–512.
24. Minot, E. D.; Yaish, Y.; Sazonova, V.; Park, J.-Y.; Brink, M.; McEuen, P. L. Tuning Carbon Nanotube Band Gaps with Strain. *Phys. Rev. Lett.* **2003**, *90*, 156401/1–156401/4.
25. Kim, D.; Lee, H.-C.; Woo, J. Y.; Han, C.-S. Thermal Behavior of Transparent Film Heaters Made of Single-Walled Carbon Nanotubes. *J. Phys. Chem. C* **2010**, *114*, 5817–5821.